New Concept to Crack Growth at High Temperature Creep and Creep-fatigue

A. T. YOKOBORI Jr.*, and T. YOKOBORI**
*Department of Mechanical Engineering II, Tohoku University, Sendai, Japan
**Tokai University, Tokyo, Japan

ABSTRACT

A new parameter, the Q* parameter is proposed for the characterization of high temperature creep crack growth. Using this parameter, the data on SUS 304 stainless steel and Cr-Mo-V steel were well characterized covering the initial or so-called tail part of da/dt diagram except the threshold part. The experimental formulation of the Q* parameter and the physical and mechanical meaning were explained. Then the relation of the Q* parameter and C* or $\dot{\Delta}$ was derived.

Finally, the Q* was shown to be applied to high temperature creep-fatigue and fatigue. For creep-fatigue, it was suggested to treat the problem as composed of the two different thermal activated processes in order to get more exact expression of the Q* parameter.

KEYWORDS

Creep; creep-fatigue; thermally activated process; C* parameter; Q* parameter; crack growth at high tmperature.

1. INTRODUCTION

A new parameter, the Q* parameter has been proposed [1, 2, 3, 7, 9] for the characterization of high temperature creep crack growth. Using this parameter, the data on SUS 304 stainless steel and Cr-Mo-V steel were well characterized covering the initial or so-called tail part of da/dt diagram except the threshold part. The experimental formulation of the Q* parameter and the physical and mechanical meaning were explained. Then the relation of the Q* parameter and C* or $\dot{\Delta}$ was derived.

Finally, the Q* was shown to be applied to high temperature creep-fatigue and fatigue. For creep-fatigue, it was suggested to treat the problem as composed of the two different thermal activated processes in order to get more exact expression of the Q* parameter.

AFR-2-BB*

2. EXPERIMENTAL FORMULATION OF Q*

da/dt versus stress intensity factor, K is experimentally measured [4, 5, 6] under constant temperature with parameter of several applied gross stress, σ_g. On the other hand, da/dt versus K is experimentally measured [4, 5, 6] under constant applied gross stress, σ_g with parameter of several temperatures. For instance, from the series of such experiments, the following experimental equation was obtained [7] for SUS 304 stainless steel:

$$\frac{da}{dt} = A_f \sigma_g^m \exp\left[-\{\Delta H_f - M\ell n(K_1/G\sqrt{b})\}/RT\right], \tag{1a}$$

or

$$\frac{da}{dt} = \{A_f \exp\left(-\frac{\Delta H_f}{RT}\right)\}\left(\frac{K_1}{G\sqrt{b}}\right)^{\frac{M}{RT}} \cdot \sigma_g^m \tag{1b}$$

where K_1 = stress intensity factor, σ_g = applied gross stress, T = absolute temperature, R = gas constant G = modulus of rigidity, b = Burgers vector, m, A_f, ΔH_f and M are constants, respectivelly. Or Eq.(1) is rewritten in the simple form as.

$$\frac{da}{dt} = A_f e^{Q^*} , \tag{2}$$

where

$$Q^* \equiv -\{\Delta H_f - M\ell n(K_1/G\sqrt{b})\}/RT\} + m\ell n\sigma_g . \tag{3}$$

Including the effect of the specimen width, W, the Eq.(1) was experimentally expressed as follows [2]:

$$\frac{da}{dt} = B\left(\frac{W}{W_o}\right)^{-\ell} \sigma_g^m \exp[-\{\Delta H_f - M\ell n(K_1/G\sqrt{b})\}/RT] , \tag{4}$$

or

$$\frac{da}{dt} = \{B \exp\left[-\frac{\Delta H_f}{RT}\right]\}\left(\frac{K_1}{G\sqrt{b}}\right)^{\frac{M}{RT}} \cdot \sigma_g^m \cdot \left(\frac{W}{W_o}\right)^{-\ell} \tag{1c}$$

where W_o = reference specimen width. Q* for Eq.(4) is written from Eq.(4) or (1c) as:

$$Q^* \equiv -\{\Delta H_f - M\ell n(K_1/G\sqrt{b})\}/RT + m\ell n\sigma_g - \ell \cdot \ell n\left(\frac{W}{W_o}\right) , \tag{5a}$$

or rewriting,

$$Q^* \equiv \frac{M\ell n\left(\frac{K_1}{K_r}\right)}{RT} + m\ell n\sigma_g - \ell \cdot \ell n\left(\frac{W}{W_o}\right) . \tag{5b}$$

where $Kr = G\sqrt{b} \exp(\Delta H_f/M)$.

In this way, Q* parameter for da/dt at the stage II was proposed in terms

of independent variables including stress intensity factor K_1, applied gross stress σ_g, temperature (absolute) T and the specimen width W, etc. in explicitly analytical term [1, 2, 3]. Uing Q* parameter, da/dt is expresed as Eq.(2).

Q* representation is well in agreement with experimental data including many data in literatures for SUS 304 stainless steel [2, 7] (Fig.1). Numerical values for ℓ, m, ΔH_f, M experimentally obtained and the values of G, b and R are substituted in Eq.(5b) and Q* thus obtained is shown in SI unit in absscisa in Fig.1.

For the case of Cr-Mo-V steel CT specimens corresponding to VAMAS Project TWP 11 [8, 12], Q* representation is also well in good accordance with the results of JSPS round robin tests as shown in Fig.2. It can be seen that Q* parameter fits much better than C* parameter as compared Figs.2 and 3, and much more than by K as shown in Fig.4. In Fig.5 the results of both round robin tests [8] by JSPS and ASTM are plotted against Q* parameter. Also, it can be seen that Q* parameter fits the data much better than C* for this case.

The numerical values were obtained experimentally in such way as mentioned above and Q* thus obtained is shown in SI unit in absscisa in Figs.2 and 5. For the case of Cr-Mo-V steel, we can see M in Eq.(3) is a linearly decreasing function of temperature, that is, $M = \alpha_1 - \alpha_2 T$, other being of quite the same type of equation as Eq.(3). (See §4)

3. PHYSICAL AND MECHANICAL MEANING OF Q* PARAMETER AND EVALUATING METHOD OF Q*

Eqs.(1) and (4) were derived originaly based on the experiments, that is, Eqs.(1) and (4) are the experimental formula in that sense. On the other hand, Eqs.(1) and (4) can be estimated from the theoretical considerations as follows:

The physical meaning of the Q* parameter comes from the fact that da/dt is represented by the following thermal activation equation [1, 2, 3, 9]:

$$\frac{da}{dt} = B \exp\left[-\frac{\Delta f_1 - \Psi(\sigma_\ell)}{RT}\right] , \tag{6}$$

where Δf_1 = activation energy, σ_ℓ = local stress near crack tip, T = absolute temperature, R = gas constant, and B = constant.

The mechanical meaning of the Q* parameter is characterized by the function Ψ. Ψ is the contribution to the reduction of the activation energy by applied load, and is a monotonicaly increasing function of local stress σ_ℓ near by the crack tip. For the case of large scale yielding like creep, Ψ is assumed as also a function of global stress, σ_g [9]. Simply assuming that the effect of these stresses is expressed by $\sigma_\ell^\delta \sigma_g^\lambda$ and the function Ψ is the logarithmic type of $\sigma_\ell^\delta \sigma_g^\lambda$ just like as many cases [10], that is,

$$\Psi = \beta \ell n(\sigma_\ell^\delta \sigma_g^\lambda) \ , \tag{7}$$

where β, δ, and λ are constants, then we can write Eq.(6) as:

$$\frac{da}{dt} = B \exp\left[-\frac{\Delta f_1 - \beta \ell n(\sigma_\ell^\delta \cdot \sigma_g^\lambda)}{RT}\right], \tag{8}$$

On the other hand, σ_ℓ is represented as [9, 11]:

$$\sigma_\ell = Mo\left(\frac{K_1}{K_o}\right)^{m_1} \left(\frac{\sigma_g}{\sigma_{go}}\right)^{n_1} \ , \tag{9}$$

where Mo, Ko and σ_{go} are constants and m_1 and n_1 are numerical constants.

By using Eq.(9), $\sigma_\ell^\delta \cdot \sigma_g^\lambda$ is expressed as:

$$\sigma_\ell^\delta \sigma_g^\lambda = M_1\left(\frac{K_1}{K_o}\right)^{m^*} \left(\frac{\sigma_g}{\sigma_{go}}\right)^{n^*} \ , \tag{10}$$

where $m^* = m_1\delta$, $n^* = n_1\delta + \lambda$, and $M_1 = Mo^\delta \sigma_{go}^\lambda$.

Substituting Eq.(10) into Eq.(8), we get:

$$\frac{da}{dt} = B \exp\left[-\frac{\Delta f_1 - \Delta f_o \ell n M_1 - \Delta f_2 \ell n\left(\frac{K_1}{K_o}\right) - \Delta f_3 \ell n\left(\frac{\sigma_g}{\sigma_{go}}\right)}{RT}\right], \tag{11}$$

where $\Delta f_o = \beta$, $\Delta f_2 = \beta m^*$, and $\Delta f_3 = \beta n^*$. Taking into account of the effect of specimen width W so that M_o in Eq.(9) is affected as $M_o = \gamma\left(\frac{W}{W_o}\right)^{-\ell}$ where γ = constant, then Eq.(11) is written as:

$$\frac{da}{dt} = B \exp\left[-\frac{\Delta f_1 - \Delta f_o \ell n\gamma - \Delta f_2 \ell n\left(\frac{K_1}{K_o}\right) - \Delta f_3 \ell n\left(\frac{\sigma_g}{\sigma_{go}}\right) + \Delta f_4 \ell n\left(\frac{W}{W_o}\right)}{RT}\right], \tag{12}$$

where $\Delta f_4 = \beta\ell$ and W_o = reference specimen width. It Δf_3 and Δf_4 are proportional to T as mRT and rRT, respectivelly, Eq.(12) is written as:

$$\frac{da}{dt} = B \exp\left[-\frac{\Delta f_1 - \Delta f_o \ell n\gamma - \Delta f_2 \ell n \frac{K_1}{K_o}}{RT} + m\ell n\sigma g - r\ell n\left(\frac{W}{W_o}\right)\right]. \tag{13}$$

4. COMPARISON OF THE Q* PARAMETER FOR SUS 304 STAINLESS STEEL AND FOR Cr-Mo-V STEEL

The reason why the exponent of σ_g is negative for Cr-Mo-V steel may be interpreted as follows: According to our analysis of the Q* parameter, $\frac{da}{dt}$ is generally affected by both local stress, σ_ℓ and global stress, σ_g. For the case of Cr-Mo-V steel, the experiment [3] shows $\frac{da}{dt}$ is proportional to K^ξ as affected by local stress field, σ_ℓ and is also proportional to σ_g^m as affected by global stress, σ_g as shown in Eq.(1), although for SUS 304 stainless steel, on the contrary, the global stress field, σ_g affects $\frac{da}{dt}$ as σ_g^m, m being positive. That is, in Eq.(1) as the basis of Q* parameter, the value of m may change according to materials. On the other hand, if the coefficient M in Eq.(1) is a linearly decreasing function of temperature for Cr-Mo-V steel as mentioned [6] in §2, it can be seen the reason why in Q* the coeffocoemt of ℓnK includes the term independent of temperature other than the term of (α_2/RT) ℓnK.

5. REPRESENTATION OF THE TAIL PART OF $\log\frac{da}{dt}$ VERSUS logC* or log$\dot{\Delta}$ or logK CURVE

In many cases the tail part of log da/dt vs logC* or log $\dot{\Delta}$ or logK curve experimentally obtained shows the curve the tangent of which is decreasing or often shows the protruding or the nose like part, which are characterized by neither C* nor $\dot{\Delta}$, nor K. Concerning the protruding or the nose like part, the cause of its appearance has been attempted to explain in terms of the relation between the characteristics of crack length a and the displacement Δ of the crack tip with respect to time [12]. On the other hand, concerning the part of the curve the tangent of which is decreasing, it is to be noted that the data covering this tail part except the threshold part are all included in Figs.1, 2 and 5, and are characterized by the Q* parameter for both SUS 304 stainless steel and Cr-Mo-V steel.

6. THE RELATION BETWEEN THE Q* PARAMETER AND C* OR $\dot{\Delta}$ PARAMETER

The displacement rate of $\dot{\Delta}$ is expressed by the thermally activated equation as follows [3]:

$$\dot{\Delta} = A_p \exp\left[-\{\Delta H_p - \phi_p(\sigma_g)\}/RT\right] . \tag{17}$$

On the other hand, $\frac{da}{dt}$ is expressed by Eq.(1), that is, the following equation of the Arrhenius type:

$$\frac{da}{dt} = B\, \sigma_g^m \left(\frac{W}{W_o}\right)^{-\ell} \left[-\{\Delta H_f - \phi_f(\sigma_g)\}/RT\right] . \tag{18}$$

By dividing the both sides of Eq.(18) by the both sides of Eq.(17),

respectivelly, then we get:

$$\frac{da}{dt} = \frac{B}{A_p}\,\dot{\Delta}\sigma_g^m\,\left(\frac{W}{W_o}\right)^{-\ell}\,\exp\left[-\{\Delta H_o - \phi_o(\sigma_g)\}/RT\right], \qquad (19)$$

where $\Delta H_o = \Delta H_f - \Delta H_p$ and $\phi_o(\sigma_g) = \phi_f(\sigma_g) - \phi_p(\sigma_g)$. On the other hand, C* is expressed as [13]:

$$C^* \simeq \frac{n-1}{n+1}\left(\frac{W}{W-a}\right)\sigma_g\dot{\Delta}, \qquad (20)$$

where n = the exponent of Norton formula. By eliminating $\dot{\Delta}$ from Eqs.(19) and (20), we get:

$$\frac{da}{dt} = \frac{B}{A_p}\,C^*\left(\frac{W-a}{W}\right)\sigma_g^{m-1}\left(\frac{W}{W_o}\right)^{-\ell}\exp\left[-\{\Delta H_o - \phi_o(\sigma_g)\}/RT\right]. \qquad (21)$$

It can be seen from Eqs.(19) and (21) that when $\Delta H_f \simeq \Delta H_p$, $\phi_f(\sigma_g) \simeq \phi_p(\sigma_g)$ and the effect of σ_g^{m-1} or σ_g^m is very small, then $\frac{da}{dt}$ can be characterized by $\dot{\Delta}$ or C*, respectively.

Eq.(1c) is rewritten as

$$\frac{da}{dt} = Be^{Q^*} \qquad (2a)$$

Equating Eq.(2a) and Eq.(19) or (21), we get the relation between the Q* parameter and C* or $\dot{\Delta}$ parameter as follows, respectivelly:

$$Q^* = -\ell n A_p + \ell n\left[\dot{\Delta}\cdot\sigma_g^m\cdot\left(\frac{W}{W_o}\right)^{-\ell}\right] - \{\Delta H_o - \phi_o(\sigma_g)\}/RT \qquad (22)$$

and

$$Q^* = -\ell n A_p + \ell n\left[C^*\,\frac{W-a}{W}\,\sigma_g^{m-1}\left(\frac{W}{W_o}\right)^{-\ell}\right] - \{\Delta H_o - \phi_o(\sigma_g)\}/RT. \qquad (23)$$

6-a. Alternative physical meaning of C* as thermal activation process

It will be shown that C* is rather interpreted as coming from thermal activated process, but not as macroscopic energy concept, that is, the extension of the meaning of J-integral. If we denote r as the rate of some atomistic rearrangement required for occuring of time dependent plastic flow, and we consider that the displacement λ will result when this rearrangement occurs, then we get the following relation as in usual thermal activation process:

$$\dot{\Delta} = \lambda r \qquad (24)$$

where r is dependent of applied stress, but λ is not. On the other hand, if we assume the crack extension will result when this same atomistic rearrangement will occurs at the crack tip, that is, this is rate-controlling, then we may write da/dt as follows just in the same way as for the displacement rate $\dot{\Delta}$:

$$\frac{da}{dt} = \eta r \qquad (25)$$

where η is independent of applied stress. In this way $\frac{da}{dt}$ will be determined only by r, that is, $\dot{\Delta}$ from Eq.(24). Since C* in the conventional sense is equivalent to $\dot{\Delta}$, say, as shown Eq.(20), then da/dt will be determined only by C* as far as we assume this same mechanism is rate-controlling one.

6-b. C* and temperature

If we plot log $\frac{da}{dt}$ against C*, we find usually $\frac{da}{dt}$ is higher with decrease of temperature for the same value of C* [9]. According to the Q* parameter we can explain the rason for the experimental characteristics, since Eq.(21) can be written as

$$\log\frac{da}{dt} = \log C^* - \{\Delta H_o - \phi_o(\sigma_g)\}/RT + \text{constant} \qquad (26)$$

and experimental value of $\Delta H_o - \phi_o(\sigma_g)$ is usually negative [3].

7. HIGH TEMPERATURE CREEP-FATIGUE AND FATIGUE

It has been shown [9, 11] that this principle as the characterization by the Q* parameter holds for high temperature creep-fatigue and fatigue also. It is to be noted, however, that with increase of the fatigue effect, for instance, for the case of high-temperature fatigue only, the term of σ_g in Eq.(1) vanishes [9, 11]. This shows that K among local stress level will play most important role than σ_g or global stress for the case of fatigue only.

In the case of high temperature creep-fatigue and fatigue also, it has been shown [11] that the Q* parameter is a good parameter as shown in Fig.6(a), (b). In Fig.7(a), (b) the same data are plotted against C*, showing a poor agreement.

Usually, creep-fatigue multiplication experiments are carried out by using trapezoidal stress wave as shown in Fig.8. Our experiments showed that the applied stress gradient effect with time, by t_R and the constant stress holding time effect by t_H are quite different on fracture life [14] and da/dt [15]. Expamples for fracture life are shown [14] in Figs.9 and 10. Similar results were obtained for $\frac{da}{dt}$ [15] (Fig.11). From these studies, it is shown that in creep-fatigue condition as in Fig.12, the two different time effects are involved, that is, the time effect 1 in process 1 and the time effect 2 in processes 1 and 2, as illustrated in Fig.12. The time effect 1 corresponds to the stress gradient with respect to time, which may be called as "fatigue effect." On the other hand, the time effect 2 reveals as the stress-time integral, which may be called as "creep effect." However, the crack growth process in high temperature fatigue appears to be

expressed in terms of Arrehenius type [17], and thus each of both process 1 and process 2 may be thermal activated process, although different process. Therefore, in these cases, in order to get more exact value of Q* parameter, it is desirous to treat the problem as composed of the two thermal activated processes.

Of course, for the case of not so high temperature, the phenomena will be controlled by both time and the number of repeated cycles, as is shown in corrosion fatigue [16]. It is interesting to note that for the case of corrosion fatigue the effect of t_R and t_H was found [16] to be quite different on da/dt.

8. SUMMARY AND CONCLUSIONS

(1) Usual criterion, such as the C* or $\dot{\Delta}$ criterion for high temperature creep crack growth rate is based on the assumption that the creep deformation rate is the rate-determining in crack growth process. However, the crack growth process is the one in which the opposed atoms are broken off or slip off each other, not the deformation process itself. On the other hand, both crack growth process and creep deformation process are thermally activated process, respectivelly. Therefore, unless a proper activation energy and the function as the activation energy decrease by applied stress are equal, respectivelly, the rate-determining process is not identical for crack grow and creep deformation. Therefore, the study is needed for a high temperature creep crack growth model in relation to the creep deformation rate.

(2) On the line of consideration (1) mentioned above, a new parameter, the Q* is proposed. By the Q* parameter the high temperature creep crack growth is well characterized than by any other parameters, such as C*, $\dot{\Delta}$ or K. Another merit of the Q* parameter is that the parameter can be estimated in terms of directly explicit representation by independent variables, such as stress intensity factor, temperature, specimen width, etc.

(3) The Q* corresponds to the exponent of the thermally activated processs equation for $\frac{da}{dt}$. Mechanical meaning of the Q* is also explained.

(4) By using the Q* parameter, the tail part of log da/dt versus log C* or log $\dot{\Delta}$ or logK curve, the tangent of which is decreasing, is well characterized being included in the whole part of da/dt curve, whereas it is not by any other parameters, such as, C*, $\dot{\Delta}$ or K.

(5) The relation between the Q* parameter and C* or $\dot{\Delta}$ parameter are derived. This equation may be a clue to develope a high temperature creep crack growth model in relation to the creep deformation rate, as suggested in (1) among these conclusions.

(6) This principle as characterization for high temperature creep by the Q* parameter holds for high temperature creep-fatigue and fatigue. The agreement with the experimental data is much more excellent as compared with by any other parameters, such as, C*, $\dot{\Delta}$ or K.

On the other hand, for the case of creep-fatigue and fatigue, in order

to get more exact value of the Q*, it is desirous to treat the problem as composed of the two thermal activated processes.

ACKNOWLEDGEMENT

The authors make their hearty thanks to all the participants of 129 Committee, JSPS who carried out the VAMAS cooperative round robin tests. Also they wish to express many thanks to ASTM and Prof. A. Saxena, the chairman of US VAMAS TWA group for using the VAMAS round robin data by ASTM.

REFERENCES

1 Yokobori, A.T., H. Tomizawa and H. Sakata, (1983) Trans of the ASME J. Engng Mater and Tech. Vol.105, p.13.
2 Yokobori, A.T. Jr., T. Yokobori, T. Kuriyama, T. Kako and Y. Kaji, (1986) Proc. Int. Conf. Creep, JSME, IME, ASME, ASTM, p.135.
3 Yokobori, A.T. Jr., H. Tomizawa, H. Sakata and T. Kuriyama, (1987) Engng Fracture Mech., 28, p.805.
4 Yokobori, T. and H. Sakata, (1980) Engng Fracture Mech., 13, p.509.
5 Yokobori, T., H. Sakata and A.T. Yokobori, Jr, Engng Fracture Mech. (1980) Vol.13, p.523.
6 Yokobori, A.T. Jr., T. Nishihara and T. Yokobori, To be published.
7 Yokobori, T., H. Sakata and A.T. Yokobori, Jr., (1980) Engng Fracture Mech. Vol.13, p.533.
8 VAMAS TWP REPORT (1988), Verailles Project on Advanced Materials and Standards
9 Yokobori, T., A.T. Yokobori, Jr., H. Sakata and I. Maekawa (1981). Three-dimensional Constitutive Relations and Ductile Fracture. (S. Nemat-Nasser, Ed.), North-Holland Pub. Co., London. U.K. p.365.
10 Yokobori, T. (1981) Advances in Fracture Research, Proc, ICF 5, (Francois, Ed.) Vol.3, p.1145.
11 Yokobori, T. and A.T. Yokobori, Jr., (1985) Advances in Fracture Research Proc. ICF 6 (S.R. Valluri, D.M.R. Tapin, P. Rama Rao, J.F. Knott, Ed.), Vol.1, Pergamon Press, Oxford. p.273.
12 Yokobori, A.T. Jr. and T. Yokobori, (1988) Engng. Fracture Mech. (In Press).
13 Koterazawa R. and T. Mori, (1977) Trans. ASME. J. Engng Mater and Tech. 99, p.298.
14 Yokobori, A.T. Jr., T. Kuriyama, Y. Kaji and T. Yokobori, (1986) J. Japan Soc. Strength & Fracture, Vol.21, No.1, pp.25-32.
15 Yokobori, A.T. Jr., Y. Kaji, T. Kuriyama and T.Yokobori, (1988) Trans. Japan Soc. Mech. Engrs, Vol.54, No.503, p.1304.
16 Yokobori, A.T. Jr., T. Yokobori, T. Kosumi and N. Takasu, (1986) Corrosion Cracking, (V.S. Goel, Ed.) Am. Soc. Metals p.1.
17 Yokobori, A.T. Jr., T.Yokobori and T. Kuriyama, (1987) ASTM STP No.942, p.236.
18 Yokobori, T., T. Kawasaki and M. Horiguchi, (1976) The Third National Conference on Fracture at Law Tatry, Slovakia.
19 Kawasaki, T. and M. Horiguchi, (1977) Engng. Frac. Mech. Vol.9 p.879.
20 Ohji, K., K. Ogura, Y. Katada, M. Takamoto and H. Nakajima, (1978) Japan Soc. Mech. Engns. Vol.27, p.1089.
21 Ohtani, R. and A. Nitta, (1976) J. Soc. Mats. Sci. Japan, Vol.25, p.746.

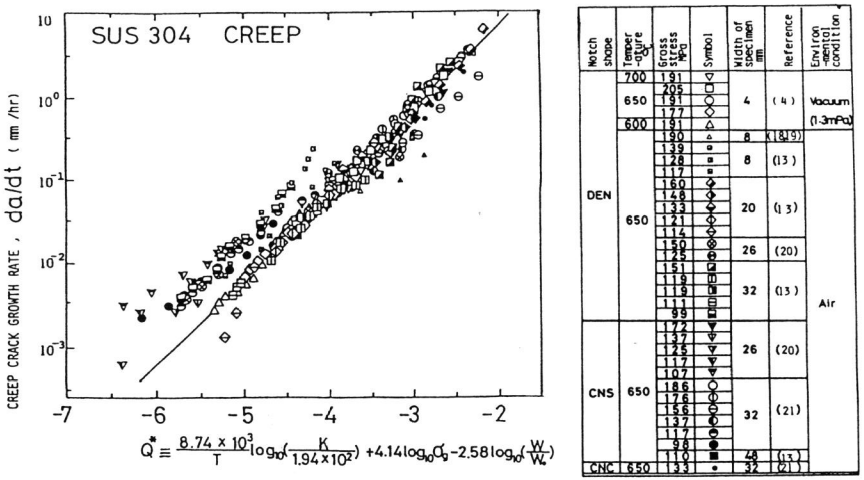

Notch shape	Temper -ature T	Gross stress σ_g MPa	Symbol	Width of specimen mm	Reference	Environ -mental condition
DEN	700	191	△	4	(4)	Vacuum (1.3mPa)
	650	205	□			
		191	○			
		177	◇			
	600	191	△			
	650	190	△	8	(18,19)	Air
		139	▫	8	(13)	
		128	▪			
		117	▪			
		160	◆	20	(13)	
		148	◆			
		133	◆			
		121	◆			
		114	◆			
		150	⊗	26	(20)	
		125	⊕			
		151	▦	32	(13)	
		119	▦			
		119	▦			
		111	▦			
		99	▦			
CNS	650	172	▼	26	(20)	
		137	▽			
		125	▽			
		117	▽			
		107	▽			
		186	○	32	(21)	
		176	⊕			
		156	⊕			
		137	◐			
		117	◐			
		98	●			
CNC	650	110	■	48	(17)	
		133	•	32	(21)	

Fig 1 da/dt as plotted against Q^* parameter (SUS 304 steel) Ref(2)

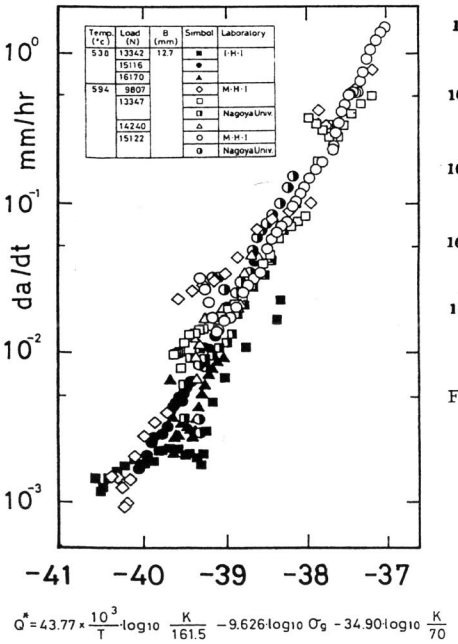

Fig 2 (da/dt) characterized by Q^*parameter Ref(6,8)

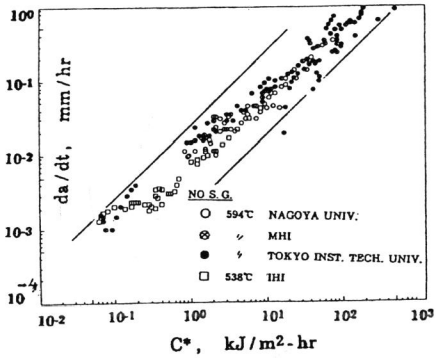

Fig 3 da/dt characterized by C* Ref(8)

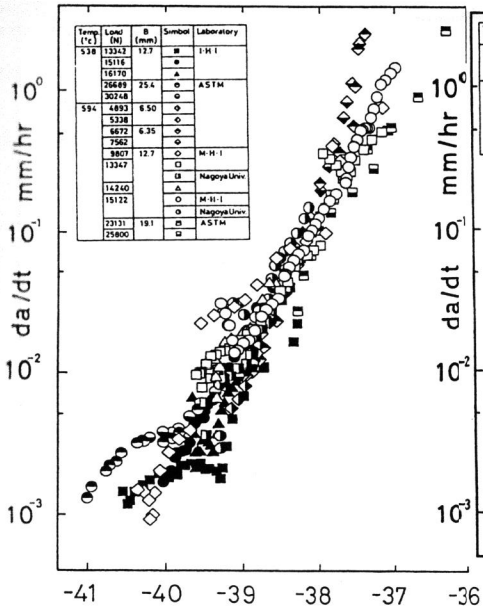

Fig 5 (da/dt) characterized by Q^*parameter Ref(6,8)

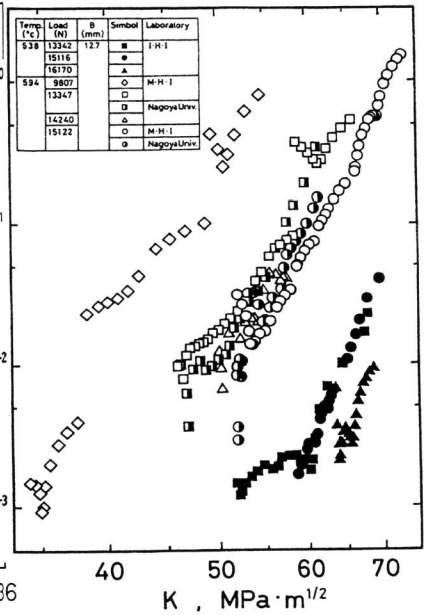

Fig 4 (da/dt) versus stress intensity factor , K Ref(6,8)

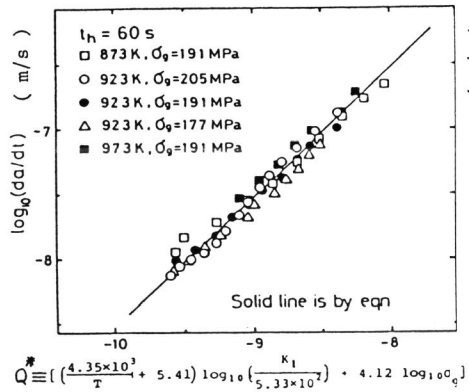

Fig.6(a) Representation of the creep-fatigue interaction crack growth rate by the Q^* parameter. t_H=60s. SUS 304 Stainless steel, Ref(9,11)

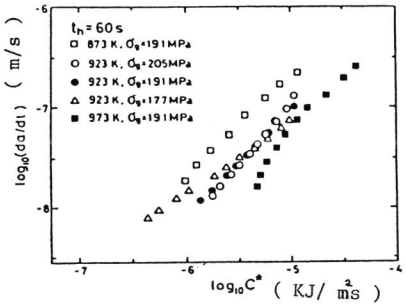

Fig 7(a) Representation of the creep-fatigue interaction crack growth rate by the C^*parameter. t_H=60s. The data are the same as in Fig.6(a) SUS 304 Stainless steel Ref.(9,11)

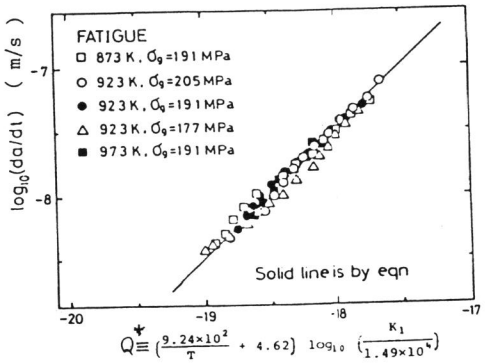

Fig.6(b) Representation of the fatigue crack growth rate by the Q^* parameter. t_H=0s. SUS 304 Stainless steel Ref(9,11)

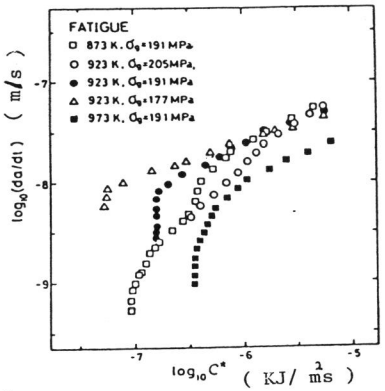

Fig 7(b) Representation of the fatigue crack growth rate by the C^* parameter. The data are the same as in Fig,6(b). Ref(9,11)

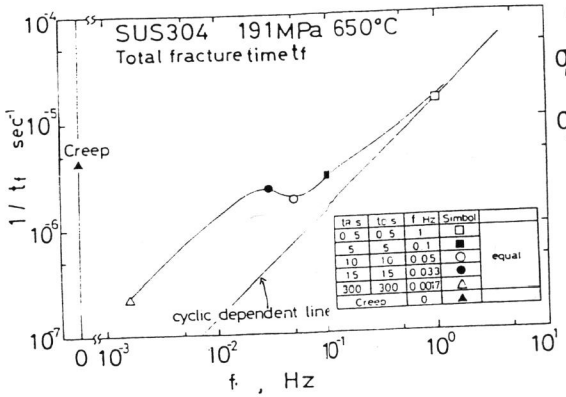

Fig 9 Effect of t_R or t_D as a measure of stress increasing or decreasing rate on the fracture life t_f under high temperature fatigue (t_H=0s). f=frequency. Ref(14)

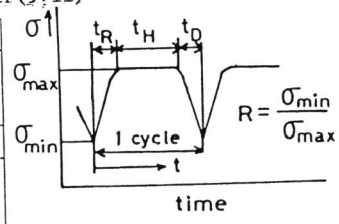

Fig 8 Stress wave used.

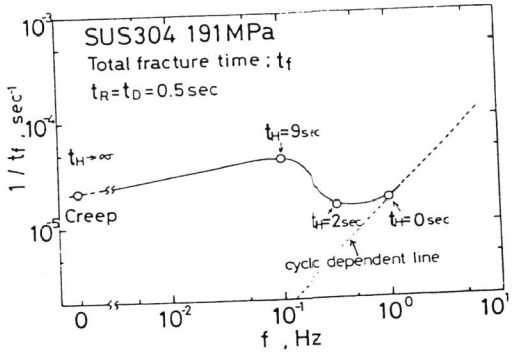

Fig 10 Effect of stress hold time t_H on the fracture life t_f under high temperature creep-fatigue. f=frequency. Ref(14)

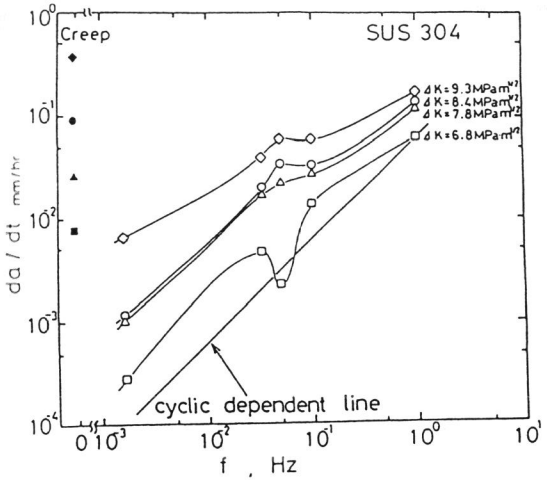

Fig 11 Effect of t_R or t_D as a measure of stress increasing or decreasing rate on da/dt under high temperature fatigue. (t_H =0s, t_R = t_D). f=frequency. Ref.(15)

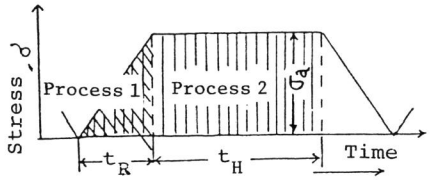

Time effect 1 involved in Process 1

Time effect 2 involved in both Process 1 and 2

Fig 12 Schematic illustration of how the Process 1 and 2 are different with respect to time effect. Ref(16)

Keynote paper presented at ICF-7, Houston, Texas,1989